

Optimization of pH-Dependent Efficiency of Ethylenediamine Tetraacetic Acid Functionalized Magnetic Nanoparticles for Total Dissolved Solids and Hardness Removal from Wastewater

Shweta Patel ¹ , Ajay Kumar Gupta ^{2,*} 

¹ Department of Chemistry, Mehsana Urban Institute of Sciences, Ganpat University, Ganpat Vidyanagar, Mehsana – Gozaria Highway, Kherva - 384012, Dist. Mehsana, Gujarat, India; shweta91047@gmail.com;

² Centre for Advanced Research Studies, Ganpat University, Mehsana – Gozaria Highway, Kherva - 384012, Dist. Mehsana, Gujarat, India; ak Gupta25@hotmail.com;

* Correspondence: director.research@ganpatuniversity.ac.in;

Received: 1.08.2024; Accepted: 3.10.2024; Published: 25.11.2025

Abstract: The use of nanotechnologies in water purification and recycling presents a theoretically and potentially promising solution that may help prevent future water shortages. Nanocomposites made from iron oxide nanoparticles exhibit excellent properties, including optical and physicochemical characteristics, magnetic recovery, and recyclability. This article highlights the role of pH in the surface charge density of nanoparticles and its effect on salt adsorption properties, which make these nanocomposites useful for the removal of total dissolved solids (TDS) and hardness from wastewater treatment. Synthesis of surface-engineered charged iron oxide nanoparticles by a simple coprecipitation method provides strong negatively charged surfaces that aid in the attraction and immobilization of oppositely charged ions in water, thereby facilitating desalination. The study involves characterizing the prepared magnetic nanoparticles using Fourier transform infrared spectroscopy (FT-IR), UV-Vis spectroscopy, dynamic light scattering (DLS), X-ray diffraction crystallography (XRD), and vibrating sample magnetometry (VSM). At room temperature, synthesized nanoparticles had an average size of 83 nm, high magnetization saturation (65.4 emu g⁻¹), and high total dissolved solids (TDS) and total hardness reduction capabilities (up to 50%). Nanoparticles can also selectively capture cations, such as Ca²⁺, Mg²⁺, etc., from the effluent, removing the ions responsible for hardness. A comprehensive analysis was conducted over a pH range of 2-10 to understand their influence on the chelation ability of the binding salts. After treatment, the magnetic nanoparticles can be easily separated from the effluent using a strong external magnet. The pre-treatment of wastewater using nanoparticles from our research can help achieve zero liquid discharge (ZLD) in effluent treatment plants.

Keywords: iron oxide nanoparticles; surface charge; cation removal; desalination; water purification; total hardness; zero liquid discharge.

© 2025 by the authors. This article is an open-access article distributed under the terms and conditions of the Creative Commons Attribution (CC BY) license (<https://creativecommons.org/licenses/by/4.0/>), which permits unrestricted use, distribution, and reproduction in any medium, provided the original work is properly cited. The authors retain copyright of their work, and no permission is required from the authors or the publisher to reuse or distribute this article, as long as proper attribution is given to the original source.

1. Introduction

The scarcity of fresh water is becoming more severe due to increasing global population demands and exacerbated by climate change [1]. Water-related challenges, such as pollution from various sources, are projected to worsen in the coming decades. As industrialization,

population growth, and natural disasters continue to impact water quality, the need for effective purification methods becomes increasingly urgent. Among the contaminants found in wastewater, heavy metals pose a significant threat to both the environment and human health. Traditional water treatment methods are insufficient to address contamination from pollutants introduced through rainfall and surface runoff [2,3]. Green nanotechnology has the potential to deliver the benefits of nanomaterials across various stages of commodity production, without the end products themselves being entirely based on nanotechnology [4,5]. Nowadays, deep learning applications are available in urban water systems, including water demand forecasting, leakage and contamination detection, sewer defect assessment, wastewater system prediction, asset monitoring, and urban flooding [6,7]. Saline water, naturally occurring and produced by various industries, including oil and gas, textiles, food, and pharmaceuticals, was traditionally disposed of but is now viewed as a valuable resource due to its environmental impacts. A new approach advocates shifting from disposal to resource recovery. Brine contains freshwater, salts, minerals, metals, chemicals, bioactive compounds, and energy potential. Minimal Liquid Discharge (MLD) and Zero Liquid Discharge (ZLD) systems are used to treat and recover these resources [8,9].

Nanotechnology also offers innovative nanomaterials to purify surface water, groundwater, and contaminated wastewater from various sources. Its advancements have revolutionized fields like engineering, physics, and chemistry. The primary applications include nano zero-valent iron, nanofiltration, nanoclays, nanobiocides, nanoadsorbents, etc. [10]. Nanomaterials, such as nano-adsorbents, photocatalysts, nano-metals, and nanomembranes, have demonstrated their effectiveness in removing toxic metallic ions, organic and inorganic solutes, and microorganisms from surface, ground, and wastewater [11,12]. Researchers are actively working on water purification methods to improve water quality and enable reuse, particularly in agriculture. Various techniques, including nanofiltration, reverse osmosis, ion exchange, membrane filtration, evaporation, and such treatments, have been explored [13].

Magnetite nanoparticles (MNPs) serve a diverse array of purposes, including magnetic separation [14] in various industries and the creation of polymer suspensions for biomedical and life science applications [15,16]. Modifying MNPs with different stabilizing agents results [17] in the production of uniform nanopowders and facilitates tailored interactions with molecules [18], thanks to specific functional groups [19], catering to a range of application needs [20,21]. Various conventional techniques for wastewater treatment using nanoparticles include chemical precipitation, membrane separation, foam separation, reduction, and ion exchange. Each of these methods has its own limitations. However, the most versatile and widely used method for wastewater treatment is adsorption [22]. Adsorption is favored for its cost-effectiveness, simplicity, effectiveness, and ease of use. Researchers have been motivated to investigate different adsorbent materials to improve the efficiency and cost-effectiveness of wastewater treatment processes [23].

Patent WO2013074669A1 describes the formation of films and filters from nanoparticles having a core surrounded by a ligand [24]. These films are made by using a nanoparticle solution after evaporating the liquid. The film primarily focuses on the rejection of larger particles from the membrane pores. Patent WO2015177391A1 describes a new nanostructured electrolyte based on magnetic iron oxide nanoparticles that provides high osmotic pressure for use in seawater or continental water purification processes through direct/forward osmosis [25]. Liu *et al.* have developed humic acid-coated Fe₃O₄ Magnetic

Nanoparticles for the efficient removal of heavy metals from wastewater [26]. The article describes the absorption of heavy metals, especially divalent or trivalent ions, in small quantities, i.e., only 10 % w/w of the nanoparticles. Patent CN102423696A describes the humic acid-modified nano-ferroferric oxide, which can be applicable for the treatment of oil-containing wastewater. The patent discussed methods for separating water from oil-containing wastewater by treating the wastewater with humic acid-modified nanoferric oxide [27].

This research paper aims to explore the potential of functionalized iron oxide nanoparticles as an innovative approach for removing TDS and hardness from wastewater. This study investigates the impact of pH on the functionalization of magnetic nanoparticles for the removal of TDS and hardness from wastewater. By functionalizing the nanoparticle surface with specific functional groups, we hypothesize that their adsorption and ion-exchange capabilities can be tailored to selectively target and remove dissolved cations and hardness-causing ions from wastewater streams. Through systematic investigations and optimization of nanoparticle synthesis, surface modification, and adsorption/ion-exchange mechanisms, this study aims to develop an efficient, cost-effective solution to address the challenges posed by TDS and hardness in wastewater treatment. In this paper, we have developed, to the best of our knowledge, a chemical process-based nanoparticle system that operates without external energy to remove positively charged ions (i.e., cations) from effluent. The nanoparticles in the present study have characteristics such as small size, negative surface charge, high negative surface charge density, magnetic properties for easy separation, and good binding affinity for ions, making them efficient at removing a large number of ions at once. Also, the nanoparticles can be regenerated and reused, making them cost-effective for industrial and seawater desalination. In addition, the nanoparticles in the present study are easy to manufacture, scalable, and user-friendly. These characteristics make them novel for their use in wastewater treatment [28].

2. Materials and Methods

2.1. Materials and instruments.

Iron salts such as Crystalline Anhydrous FeCl_3 (98%), $\text{FeSO}_4 \times 7\text{H}_2\text{O}$ (97%) were purchased from Chemdyes Co. NaOH (97%) was purchased from Molychem. EDTA disodium salt (98%) was purchased from Fisher Scientific, India. Distilled water was collected from an in-house double distillation unit. All the Glasswares were calibrated before use. Instruments such as Magnetic stirrer (REMI-5MLH, Mumbai, India) and micro-pipette (VAR VOL 100–1000 μl , Kasablanka-Mumbai, India), Microwave Oven (frontline Instruments, New Delhi, India), Weighing Balance (Scale tech, Pune, India), pH meter and Conductometer (Systronics Instruments, Ahmedabad, India), Centrifuge (REMI-5000 RPM, Mumbai, India) were calibrated before their use.

2.2. Synthesis of ethyl diamine tetraacetic acid (EDTA) coated iron oxide nanoparticles (IONPs).

2.2.1. Synthesis of Iron oxide nanoparticles (IONPs).

The bare iron oxide magnetic nanoparticles were synthesized using a simple co-precipitation method modified from references [29,30], as illustrated in Figure 1. A solution containing a 1:2 ratio of Fe^{2+} and Fe^{3+} ions was gradually added to double-distilled water while

stirring constantly. 1.0 M NaOH was slowly added under continuous stirring, and the solution's pH was adjusted between 10 and 11. The mixture was stirred for 1 hour for homogenization and completion of the reaction. The resulting IONPs were separated using a permanent magnet, washed multiple times with deionized water, and then dried in an oven at 70°C for 24 hours. The dried sample was stored in an airtight container at ambient temperature for further analysis [31].

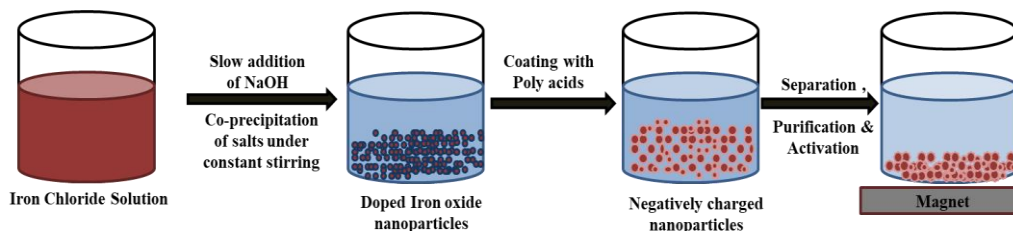


Figure 1. Schematic presentation of the synthesis of coated IONPs.

2.2.2. Surface modification of IONPs with EDTA.

After the temperature of the synthesized nanoparticles was reduced to 40°C, 10 g of EDTA-disodium salt was added and stirred for 3 hours at room temperature using a magnetic stirrer. Surface modification of the nanoparticles was performed by neutralizing them with 0.01 M HCl under continuous vigorous stirring at room temperature [32,33].

2.3. Activation of nanoparticles.

Synthesized EDTA-coated IONPs were washed multiple times with double-distilled water. The nanoparticle suspension was activated for wastewater treatment by maintaining total dissolved solids (TDS) at 30 ppm and pH at 3. pH adjustment is crucial to maintain optimal conditions for adsorption, while characterization and optimization ensure effective surface modification. Overall, activation processes to obtain nanoparticles with low TDS and pH can effectively treat wastewater, offering a promising solution for water remediation in challenging environmental conditions.

2.4. Spectroscopic studies.

2.4.1. UV-Vis spectroscopy for iron concentration determination.

UV-Vis spectroscopy (Shimadzu UV-1900, Kyoto, Japan) was performed to determine the ion concentration using FeCl₃; the known amount of particles was dissolved in concentrated HCl and incubated for 2 hours at 50° to 60°C. The spectrophotometric measurements were performed at 334 nm using a UV-Vis spectrophotometer [34].

2.4.2. Fourier transformed infrared (FTIR) spectral studies.

The EDTA coatings on IONPs were analysed by FT-IR spectroscopy to confirm the successful attachment of EDTA to the NP surface. This technique provides detailed information about molecular vibrations and chemical bonds within a sample, verifying the presence of specific functional groups associated with the polyacid coating [35].

2.5. Characterization of IONPs.

2.5.1. Measurement of particle size.

The particle size of the different nanoparticle samples was determined by dynamic light scattering (DLS) using a HORIBA Scientific nano PARTICA SZ-100 (HORIBA Scientific, Kyoto, Japan). The samples were prepared by dispersing NPs in double-distilled water to form a stable colloidal suspension, and sonication was applied as needed to ensure uniform dispersion. During the measurement, a laser beam was centered on the sample, and different angles of scattered light were measured. The hydrodynamic diameters of the NPs were determined by analyzing the intensity variation of the scattered light. The particles were then processed to generate an accurate size distribution profile [36].

2.5.2. X-ray diffraction.

XRD studies were done with dry crystalline nanoparticles using (Philips-PW1800, Eindhoven, Netherlands) with $\text{CuK}\alpha$ radiation ($\lambda = 1.54184 \text{ \AA}$) - range of 20° - 80° with a step size of 0.02° . For XRD studies, finely powdered NPs were prepared and pressed into a flat sample holder to ensure a smooth and even surface. As the X-ray interacted with the crystalline planes of the NPs, a diffraction pattern was recorded, consisting of peaks corresponding to different crystallographic planes. The intensities and positions of different peaks provided detailed information about the crystalline structure and phase composition of the NPs. The crystal size, d , of the synthesized samples was calculated using the Scherrer equation [37].

2.5.3. Vibrating sample magnetometry.

VSM analysis of the magnetic properties of nanoparticles was performed using a Lake Shore (7410 Series VSM 2019, Cryotronics, Westerville, USA) at room temperature. A variable magnetic field was applied to the sample, and the resulting magnetization was measured as a function of the applied field. Magnetic properties, including saturation magnetization (M_s), Coercivity (H_c), and remanence magnetization (M_r) from the hysteresis loop, were determined using the VSM technique [38].

2.6. TDS and Hardness removal studies.

2.6.1. Sedimentation studies.

Studies of IONPs sedimentation were carried out to investigate the influence of a magnetic field on their settling behavior. Two sets of experiments were performed: one with the application of a magnet and the other without it. 10% w/v nanoparticle samples were placed in a 200 ml beaker, and their settling behavior at the bottom was monitored over time [39].

2.6.2. TDS and Hardness Reduction Studies.

To assess desalination capability, an effluent with TDS around 4000 ppm, hardness around 300 ppm, and an alkaline pH between 9 and 11 was treated with NPs. pH of the nanoparticle system was around 3.0 (i.e., below the pK_a values of ionizable groups in the EDTA).

2.6.3. TDS and Hardness Reduction Experiment.

To evaluate the effectiveness of EDTA-IONPs in removing TDS from effluent, an experimental setup was designed using synthetically prepared effluent. The effluent was prepared by dissolving 3 g of NaCl in 1 L of water to achieve a TDS of 3000 ppm. Experiments were conducted with 100 ml effluent samples treated with various concentrations of 12% w/v EDTA-IONPs (at 10 to 50 ml). Experiments were performed in duplicates to ensure accuracy and reproducibility. To verify results at a larger scale, 500 ml of effluent was treated with 100 ml of nanoparticles, mixed for 10 minutes, and allowed to settle for 60 minutes. After treatment, the nanoparticles were separated by using an external magnet. This experimental setup aimed to assess the efficiency of EDTA-IONPs in TDS reduction.

An effluent with 300 ppm hardness was prepared by adding 0.4 g of $\text{CaCl}_2 \times 2\text{H}_2\text{O}$ and 0.6 g of $\text{MgCl}_2 \times 6\text{H}_2\text{O}$ to 1 liter of water and used for further hardness removal experiments. Different concentrations (10 to 50 ml) of EDTA-IONPs were added to separate aliquots of hardness effluent, thoroughly mixed, and allowed to interact with the hardness-causing ions, ensuring uniform distribution and interaction with the hardness-causing ions. The pH was adjusted to around 9 to optimize the chelation process, which involves the binding of EDTA with Ca^{2+} and Mg^{2+} ions.

2.6.4. Regeneration and reuse of nanoparticles.

The regeneration process restores the nanoparticles' functionality after they have captured TDS and hardness from the effluent, enabling reuse and enhancing economic viability. After the effluent treatment, the nanoparticles were separated from the treated effluent using a magnetic separator. The captured salts, calcium and magnesium ions, were then removed by washing the nanoparticles with 0.01 M HCl, which protonated the EDTA groups and released the bound positively charged ions. The nanoparticles were subsequently rinsed with deionized water to remove any residual acid and desorbed ions [40].

2.6.5. Effect of pH of nanoparticles and effluent.

The effect of pH on both the effluent and NPs was systematically varied from 2.0 to 10.0 to investigate its impact on TDS removal by nanoparticles. To achieve the desired pH levels, 0.1 N hydrochloric acid (HCl) and sodium hydroxide (NaOH) solutions were used. This study examined the correlation between pH variation and the efficiency of NPs in removing TDS [40,41].

2.6.6. Effect of concentration of nanoparticles.

In this study, different concentrations of NPs were used to investigate their effect on the removal of TDS from effluent. Specifically, NPs volumes ranging from 10 mL to 50 mL were added to a 100 mL sample of effluent. The initial effluent concentration was 4000 ppm, and pH was maintained around 10 to optimize interaction with the NPs, with a pH range of 1 to 3.

3. Results and Discussions

IONPs were synthesized by the simple co-precipitation method using an initial precursor solution of iron salts such as FeCl_3 and FeSO_4 . After synthesizing IONPs, they were

coated with EDTA-disodium salt to enhance their stability and functionality in TDS and hardness removal. The coating of EDTA involves the strong interaction between the surface of IONPs and EDTA molecules. EDTA, being a hexadentate ligand, has four carboxylic and two amine groups capable of binding to metal ions. The pKa values of EDTA play a crucial role in the binding efficiency of nanoparticles to different salts of opposite charge. Adjusting the wastewater solution to an alkaline pH (10-11) facilitates the deprotonation of the carboxylic group and increases the negative charge density on the EDTA molecules. EDTA forms multiple coordinate bonds with the iron and oxygen atoms present in IONPs. The chelating effect of EDTA stabilizes the nanoparticles, preventing aggregation and enhancing their dispersibility in aqueous solution. This EDTA coating not only stabilizes the IONPs but also introduces functional groups that can interact with positively charged ions from the effluent. After coating, EDTA-IONPs were washed multiple times with double-distilled water and activated by adjusting the pH to 3 using 0.01 M HCl and TDS at 30 ppm. The EDTA-IONPs, when added to water with high TDS, bind to the positively charged ions present in the effluent. The nanoparticles can then be separated by filtration, sedimentation, magnetic separation, centrifugation, or other methods, leaving behind water with significantly reduced TDS.

3.1. Spectroscopic analysis.

FTIR spectra as given in Figure 2 were employed to analyze the coating of EDTA on the nanoparticles: IONPs, EDTA-IONPs, and EDTA. The FTIR spectra showed distinct bands corresponding to Fe-O bond vibrations, observed at lower wavenumbers ($\leq 700\text{ cm}^{-1}$). Particularly, the band at 550 cm^{-1} corresponded to the stretching vibration mode of Fe-O bonds in magnetite nanoparticles (IONPs).

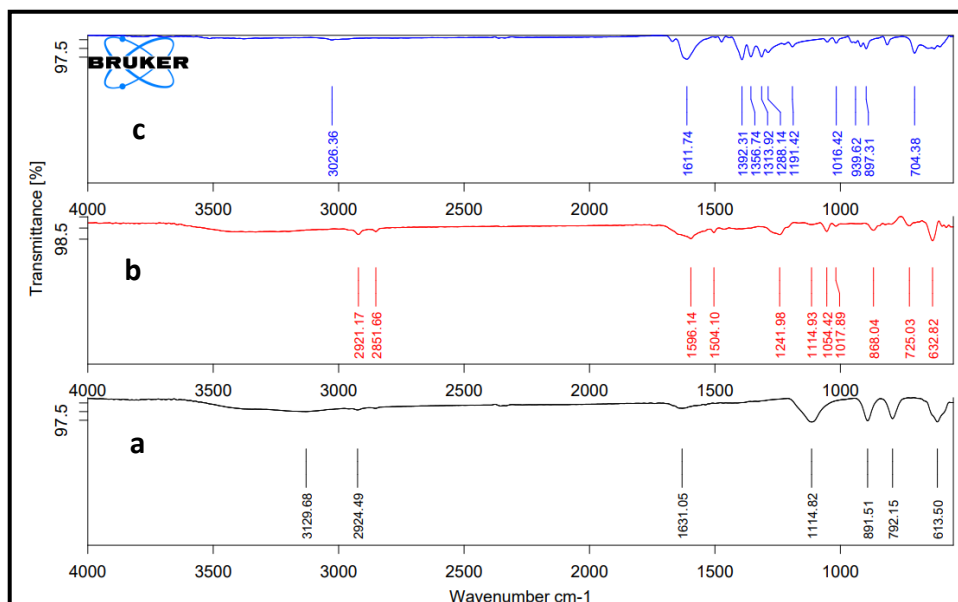


Figure 2. FTIR spectra of (a) IONPs; (b) EDTA-IONPs; (c) EDTA.

A broad absorption band in the range of $2800\text{-}3300\text{ cm}^{-1}$ suggests the presence of O-H stretching and bending vibrations, likely originating from water molecules and the O-H group of EDTA. An absorption peak within the $2800\text{-}2900\text{ cm}^{-1}$ range is attributed to the stretching vibration of C-H bonds. Two sharp peaks at 1724 and 1637 cm^{-1} correspond to C=O and C-O bonds, indicating the presence of carboxylic acid groups, as reported by Liu *et al.* [42].

The UV-Vis spectroscopy results given in Figure 3 demonstrate the successful quantification of iron content in IONPs. The reliability of the iron determination method was confirmed by a linear calibration curve with a high correlation coefficient in a standard FeCl_3 solution. The iron content was confirmed to be above 90% of the original iron salts in nanoparticle samples. The measured iron concentrations in the nanoparticle samples are consistent with the expected values, indicating efficient synthesis and coating processes.

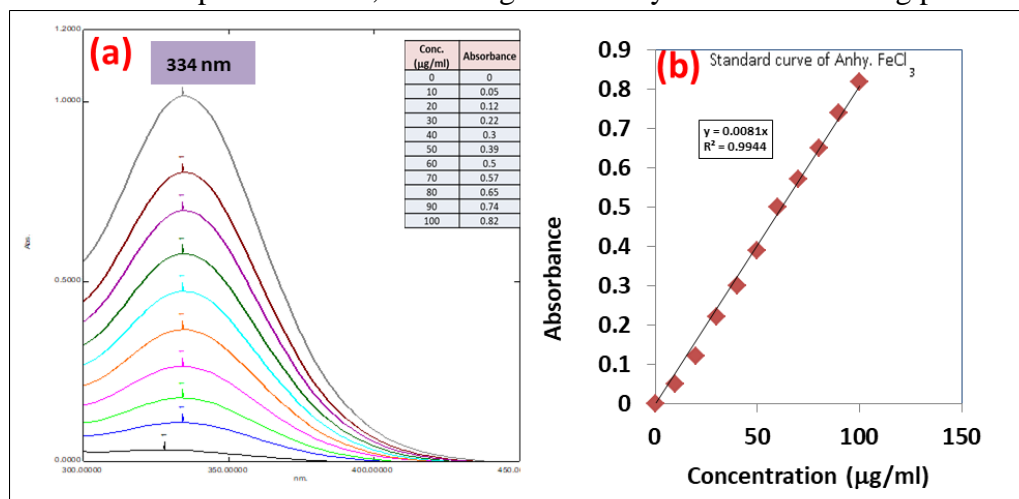


Figure 3. (a) UV-Vis spectroscopy of IONPs; (b) Standard curve of Anhy. FeCl_3 .

3.2. Particle size analysis.

Particle size analysis of IONPs and EDTA-IONPs was determined using dynamic light scattering (DLS), as shown in Figure 4. It is a powerful technique used to determine the size distribution and stability of NPs in suspension. In this study, DLS was employed to measure the hydrodynamic diameter of IONPs and EDTA-IONPs by monitoring the intensity fluctuations in scattered light caused by the Brownian motion of nanoparticles in suspension. The size of the IONPs was to be around 82 nm. After coating the IONPs with EDTA, the hydrodynamic size increased substantially to 272.5 nm. This increase in size suggests that the coating material adds layers by modifying the nanoparticles' surfaces, making them highly hydrophilic. EDTA molecules adsorb onto the nanoparticles' surfaces, forming a protective layer that stabilizes the particles and prevents agglomeration.

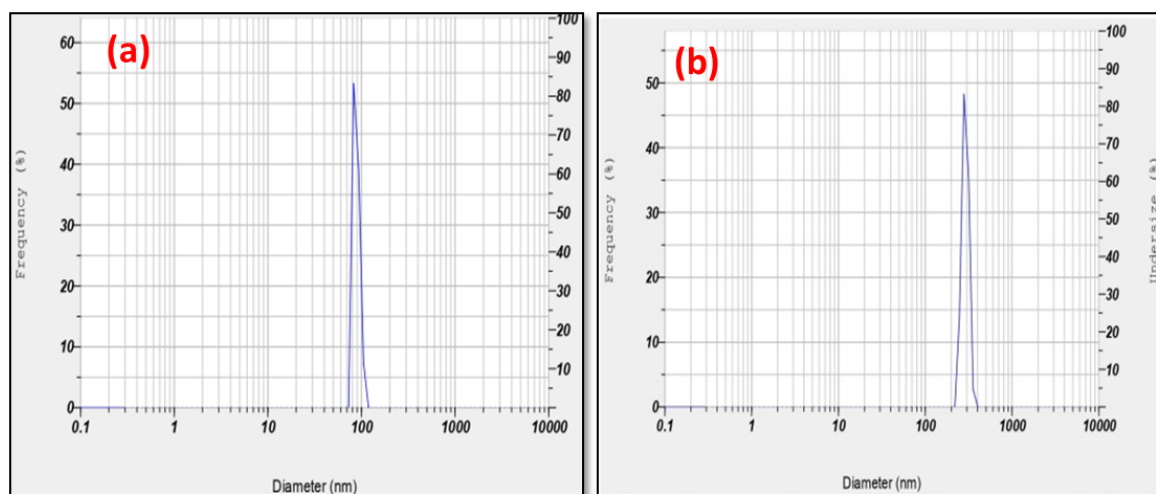


Figure 4. Particle size distribution of (a) IONPs; (b) EDTA-IONPs.

3.3. X-ray diffraction.

The crystallite orientations of the iron oxide nanoparticles were investigated using powder X-ray diffraction (XRD) in Figure 5. The X-ray diffraction pattern of the calcined powder synthesized by this method shows a clear, distinctive signature, confirming the successful formation of IONPs [43]. The size of crystalline nanoparticles was calculated using the Scherrer equation.

$$d = \frac{K\lambda}{\beta\cos\theta} \quad (1)$$

Where K = Scherer constant (0.89); λ = x-ray wavelength ($\lambda = 1.54184 \text{ \AA}$); θ ($^\circ$) = Bragg diffraction angle.

The characteristic diffraction peaks of anatase at 33.4° , 36.5° , 43.7° , 58.7° , and 62° correspond to the reflections from the (002), (113), (004), (115), and (044) planes, which were observed, and no rutile peaks were detected (Crystallographic card number JCPDS 96-900-2322).

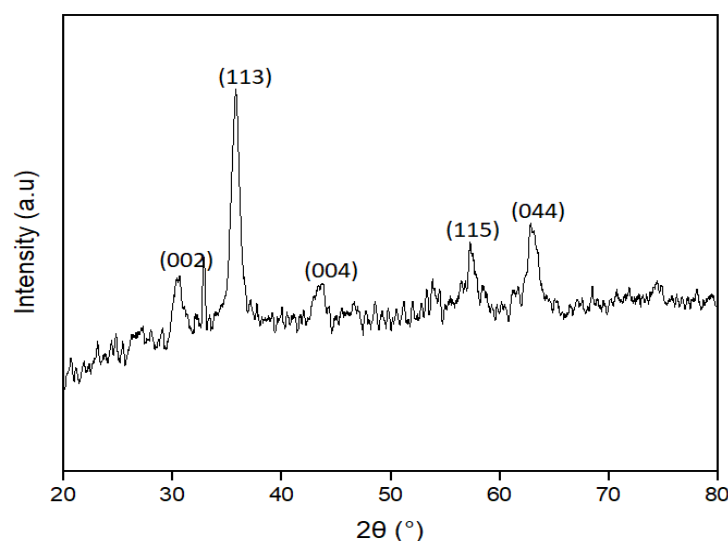


Figure 5. X-ray diffraction spectra of IONPs.

The cubic spinel structure was observed to align with the expected crystallographic configuration. No additional phases or impurities were identified in the analysis. Particle size analysis was determined using the Scherrer formula, based on the most intense peaks, yielding an average particle size of 28.98 nm.

The controlled manipulation of the rate of NaOH mixing with the salt solution is crucial for determining particle size variation. Specifically, faster mixing rates lead to the generation of larger particles, as the growth rate surpasses the nucleation rate under these conditions. This nuanced control over particle size is significant for tailoring the material's properties, making it a valuable aspect in materials science.

3.4. Vibrating sample magnetometry.

Magnetization curves at room temperature of the iron oxide and EDTA-coated Iron oxide nanoparticles are illustrated in Fig. 6. Magnetic nanoparticles exhibit superparamagnetic behavior at room temperature due to their low coercivity and remanent magnetization. The saturation magnetization of these nanoparticles was measured and found to be around 65.4

emu/g. The superparamagnetic property of magnetic nanoadsorbents is a crucial characteristic for their potential use in aqueous solutions. EDTA-IONPs functionalized magnetic nanoparticles demonstrate comparable paramagnetic properties to regular uncoated nanoparticles and show a strong response when subjected to an additional permanent magnet. This enables the rapid separation of the magnetic nanoparticles from water, making them highly effective for various applications [44]. However, no difference in saturation magnetization values was observed between EDTA-IONPs and uncoated IONPs.

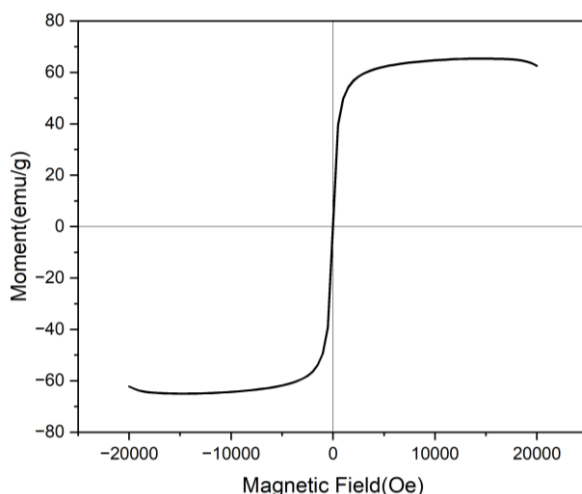


Figure 6. Magnetic hysteresis curve of IONPs.

3.5. Sedimentation studies of EDTA –IONPs.

The sedimentation study highlights the effects of magnetic fields on the sedimentation behavior of IONPs, as shown in Table 1. In this experiment, two sets of 200 mL nanoparticle suspensions were prepared and subjected to two conditions: with and without a magnet. When the nanoparticles were placed on the magnet, the sedimentation volume was measured at 1, 3, 5, and 7-minute intervals. The rapid aggregation and settling were observed in the presence of an external magnet. At 7 minutes, the sediment volume reduces to 30 ml. In contrast, without a magnet, the sedimentation rate was slower compared to the magnet-assisted condition (Table 1), and it took about 35 min to completely settle the particles [19,45].

Table 1. Sedimentation study of EDTA-IONPs using a magnet.

Sedimentation with a magnet		Sedimentation without magnet	
Time (minutes)	Sedimentation (mL)	Time (minutes)	Sedimentation (mL)
0	200	0	200
1	80	9	100
3	60	15	70
5	50	20	50
7	30	35	30

3.6. TDS reduction from effluent.

The potential of nanoparticles as a promising technology for TDS reduction in effluent treatment is shown in Figure 7. Optimization of nanoparticle dosage, pH conditions, and other treatment parameters can further enhance treatment efficiency and improve the quality of treated effluent.

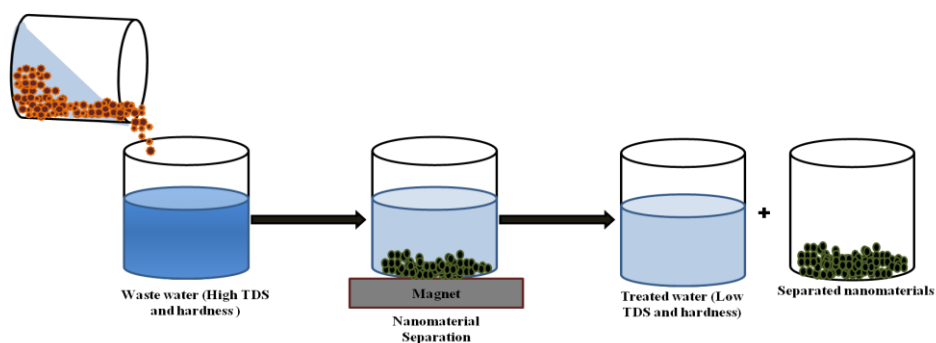


Figure 7. Application of nanoparticles in TDS and hardness removal.

100 ml of effluent samples with initial TDS values ranging from 4000 ppm to 4400 ppm were taken for the TDS reduction study. The pH of the effluent was kept around 10. Different volumes of nanoparticles (NPs) having a concentration of 12% w/v were added to the effluent samples for treatment, ranging from 10 ml to 50 ml. The pH of the nanoparticles was maintained between 1 and 3. After treatment with nanoparticles, the final TDS values decrease, indicating the effectiveness of the treatment using NPs. The percentage reduction in TDS relative to the initial TDS is calculated for each sample, and the reduction ranges from 7.3% to 53% depending on the process parameters (Figure 9b). This study highlights the importance of optimizing both the NPs dosage and pH conditions to maximize TDS removal efficiency. The results showed that adjusting these parameters can achieve significant improvements in the quality of treated effluent.

3.7. Hardness reduction from effluent.

The results indicated a significant reduction in hardness level upon treatment with EDTA-IONPs, as shown in Figure 8. The reduction in hardness can be attributed to the high affinity of the deprotonated carboxylic group of EDTA for calcium and magnesium ions. By optimizing pH and nanoparticle concentration, binding efficiency with cations can be increased. The percentage of hardness reduction compared to the initial hardness was calculated depending on such parameters. Up to a 30% reduction in hardness, and a positive correlation between nanoparticle concentration and hardness removal efficiency, underscore the importance of optimizing these parameters in practical applications to achieve the desired reduction in hardness.

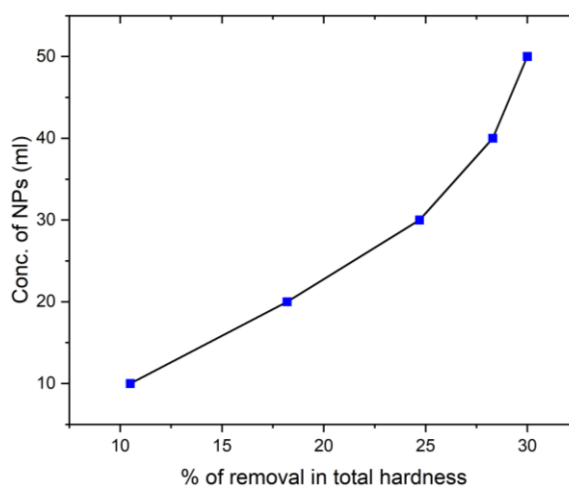


Figure 8. The graphing representation of the percentage of total hardness removal vs concentration of NPs (in millilitres).

3.8. Effect of pH on TDS and hardness removal.

The pH of EDTA-IONPs directly affects the ionization state of the functional group of EDTA, as shown in Figure 9. The pKa values of the four carboxylic groups (-COOH) of EDTA are 2.0, 2.7, 6.2, and 10.3, and two amine groups (-NH₂) with pKa values around 6.2 and 10.3. At pH below the lowest pKa of the polycarboxylic acid, the nanoparticle surfaces have the maximum negative charge. In contrast, at higher pH levels, carboxylic groups lose their protons and become deprotonated, enhancing their chelating or binding properties to capture positively charged metal ions (Ca⁺², Mg⁺²), sodium ions (Na⁺), etc. These highly negatively charged nanoparticles can easily attract the cations. This binding occurs through the formation of stable complexes between negatively charged carboxylic groups and metal ions. The pH of the effluent significantly influences the efficiency of TDS and hardness removal using EDTA-IONPs [46,47]. Effluent with an alkaline condition (pH 7-11) promotes better interaction between NPs and salts. Under acidic conditions (pH 2-6), the efficiency of TDS removal may decrease due to the protonation of EDTA's functional group, leading to weaker binding with metal ions and other dissolved species. In this experiment, synthetic effluent at 3000 ppm was treated with varying concentrations of nanoparticles (10-50 ml) at different pH levels. It was observed that effluents with alkaline pH (8-10) exhibited the highest salt reduction compared to neutral (pH 7) and acidic (pH 4-6) conditions (Figure 9) [48-50] This is due to the nanoparticles' negative surface charge in alkaline conditions [51,52], which enhances the adsorption of positively charged ions such as Ca²⁺ and Mg²⁺. Additionally, the formation of metal hydroxide complexes and increased nanoparticle aggregation in alkaline environments promote more efficient TDS removal. Thus, adjusting the effluent pH to alkaline levels optimizes the performance of EDTA-IONPs in TDS and reduces hardness.

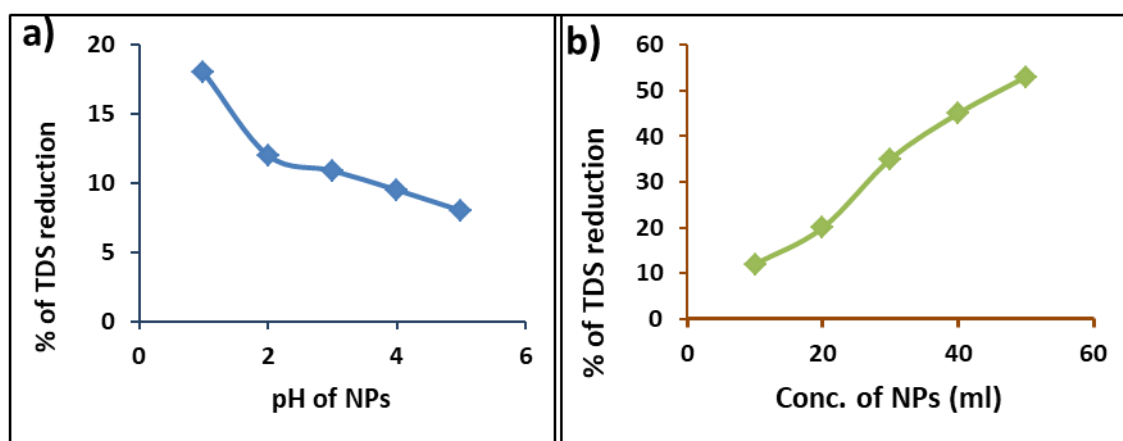


Figure 9. The graphic representation of **a)** percentage of TDS reduction vs pH of NPs; **b)** percentage of TDS reduction vs Conc. of NPs (in millilitres).

3.9. Effect of concentration on TDS and hardness removal.

The concentration of EDTA-IONPs used for effluent treatment significantly impacts the TDS removal efficiency. Higher NPs concentration increases the availability of chelation sites, improving TDS removal efficiency, but excessive amounts can cause aggregation. Figure 9 shows a positive correlation between EDTA-IONP concentration and the percentage of TDS removal in synthetic wastewater [53]. As the concentration of NPs increases from 10 mL to 50 mL, the TDS removal efficiency improves significantly (up 50%) (Figure 9). Higher concentrations result in greater TDS removal due to increased surface area, active NPs, aggregation, and synergistic effects. As the concentration of NPs increased, it was observed

that the TDS reduction efficiency also increased. The TDS reduction was 53% with 50 ml (12% w/v) NPs, whereas it was only around 7.3% with 10 ml (12% w/v) NPs. Optimizing nanoparticle concentration and pH conditions is essential for maximizing treatment efficiency, offering a promising approach to enhancing the effectiveness of nanoparticle-based wastewater treatment processes [54,55].

3.10. Regeneration and reuse of NPs.

In Figure 10, the graph of TDS Removal Efficiency (%) vs. Regeneration Cycle illustrates how the efficiency of EDTA-IONPs in removing TDS from a 4000 ppm solution changes over 10 regeneration cycles. Initially, the nanoparticles achieve a 49% TDS removal efficiency. As the number of regeneration cycles increases, this efficiency gradually decreases, reaching 44% by the 10th cycle. This reduction in efficiency is partly due to the loss of NPs and a potential decline in their active surface area over time, driven by the loss of loosely bound EDTA molecules, if any. However, even with this decrease, the nanoparticles still maintain significant TDS removal capability. By enabling multiple uses of the same batch of nanoparticles, the regeneration process substantially reduces the need for fresh nanoparticle synthesis, thereby saving on material production and resource consumption costs. Additionally, the ability to reuse nanoparticles minimizes waste generation and supports environmentally sustainable practices in water treatment applications.

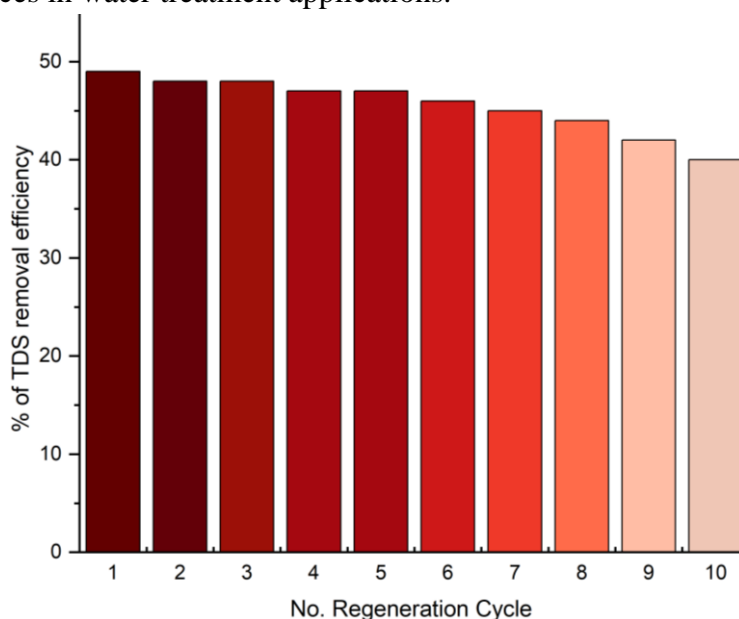


Figure 10. Graph showing the percentage of TDS removal vs No. Regeneration cycle.

In this study, iron oxide nanoparticles (IONPs) were synthesized using a co-precipitation method [56], in which metal ions were precipitated with a base at an appropriate pH. The solution was stirred to ensure thorough mixing, and the nanoparticles were magnetically separated, washed, and dried. For surface modification, the nanoparticles were treated with a chelating agent, stirred, and neutralized with an acid. The modified nanoparticles were then washed and activated for wastewater treatment by adjusting the total dissolved solids (TDS) and pH to optimal levels, enabling effective adsorption and removal of salts. The pH of EDTA-IONPs affects their charge and binding ability. At low pH, the carboxylic groups on the nanoparticles are deprotonated, and when mixed with alkaline effluent, these carboxyl groups get deprotonated. In this way, a negative charge is generated on the particle surfaces, which enhances the binding of positively charged metal ions. In this study, it was observed that

alkaline conditions (pH 7-11) improve the efficiency of TDS and hardness removal. By controlling the pH, the ionization state of EDTA can be tailored to enhance the nanoparticles' ability to bind and remove harmful cations, such as calcium, magnesium, and sodium, which contribute to high total dissolved solids (TDS) and water hardness. This provides a cost-effective, scalable, and efficient solution for industries, reducing operational costs.

4. Conclusions

This study demonstrates the significant potential of functionalized IONPs for the removal of TDS and hardness from wastewater. The synthesized nanoparticles, with an average size of 83 nm and high magnetization saturation (65.4 emu/g), were shown to be effective in reducing TDS and hardness by up to 50%. Surface modification of these nanoparticles with EDTA enhanced their ability to selectively capture cations, such as Ca^{2+} and Mg^{2+} , which are responsible for water hardness. Characterization of nanoparticles using various techniques confirms their size, nature, composition, magnetism, and functional properties. Experimental results highlighted the influence of pH and nanoparticle concentration on the efficiency of TDS and hardness removal. The findings reveal that the pH of the NPs and the effluent significantly influences the chelation ability of EDTA, with optimal performance observed at slightly alkaline conditions, where EDTA is fully deprotonated. At these higher pH levels, the nanoparticles effectively bind and remove calcium and magnesium ions, resulting in a substantial reduction in water hardness and TDS. Regeneration studies showed the NPs retained their effectiveness over multiple cycles. Increased nanoparticle concentrations further improved TDS removal efficiency, demonstrating a direct correlation between nanoparticle volume and treatment efficacy. Overall, this research underscores the viability of EDTA-IONPs as a cost-effective and efficient wastewater treatment solution. The ability to easily separate the nanoparticles from treated effluent using a magnetic field enhances the practicality and sustainability of this approach.

The outcome of this research work can be utilized in a number of industries, including textiles, chemicals, pharma, dyes and pigments, ceramics, etc. These industries discharge effluent high in dissolved organic matter, inorganic salts, and other harmful substances. In this research, we have synthesized nanoparticles for wastewater treatment that desalinate high-salinity water cost-effectively. The treated water obtained from these nanomaterials may be used as process water in industry or for irrigation. The treated water can also be converted into potable water by processing it through reverse osmosis, where our pre-treatment method using nanomaterials will enhance water recovery and significantly reduce the reject stream volume. No such effluent pre-treatment technology is currently available. Once implemented, it can be a game-changer for the water treatment industry and for areas where high-salinity water is abundant.

By efficiently removing cations and hardness from wastewater, these nanoparticles can help reduce the load of organic and inorganic contaminants, which also has the ability to influence Chemical oxygen demand (COD) and Biological Oxygen demand (BOD) levels. The improved water quality supports biological processes in ecosystems, promoting healthier aquatic environments. Future work will focus on optimizing nanoparticle synthesis and surface modification processes to further enhance the performance and scalability of this technology for real-world applications. The use of these nanoparticles would enable the effluent treatment plant to desalinate wastewater and make it suitable for reuse in the process, thereby supporting water recycling. This can also help desalinate salty and brackish water, remove water hardness,

remove toxic heavy metal ions, and purify sea, lake, and river water. This can greatly help restore depleted water sources and enable the nation to meet its clean water requirements at an economical cost.

Author Contributions

Investigation, S.P.; Conceptualization, A.K.G.; Methodology, S.P. and A.K.G.; Data curation S.P. and A.K.G.; Formal analysis, S.P. and A.K.G.; Validation, S.P. and A.K.G.; Visualization, S.P. and A.K.G.; Writing – original draft, S.P.; Writing – review & editing, A.K.G. funding acquisition, A.K.G. All authors have read and agreed to the published version of the manuscript.

Institutional Review Board Statement

Not applicable.

Informed Consent Statement

Not applicable.

Data Availability Statement

Data supporting the findings of this study are available upon reasonable request from the corresponding author.

Funding

This research work was supported by the funding from Gujarat Council on Science and Technology (GUJCOST), Department of Science and Technology, Govt. of Gujarat, India, in the form of a research project (Sanction order No. GUJCOST/STI/2023-24/253) dated 25th April, 2023.

Acknowledgments

The authors would like to acknowledge Ganpat University, Gujarat, India, for providing the laboratory facilities to conduct this research.

Conflicts of Interest

The authors declare no conflict of interest.

References

1. Lavate, S.; Kumar, S.; Seena, S.; Srivastava, R. Chapter 11 - Recent advances in environmental nanotechnology. In *Nanoparticles and Plant-Microbe Interactions*, Seena, S., Rai, A., Kumar, S., Eds.; Academic Press: **2023**; pp. 293-318, <https://doi.org/10.1016/B978-0-323-90619-7.00004-7>.
2. Nguyen, M.D.; Thomas, M.; Surapaneni, A.; Moon, E. M.; Milne, N.A. Beneficial reuse of water treatment sludge in the context of circular economy. *Environ. Technol. Innov.* **2022**, *28*, 102651, <https://doi.org/10.1016/j.eti.2022.102651>.
3. Van, D.H.L.E.; Van, N.R. Designing a sustainable water management strategy including disaster management. *IFAC-PapersOnLine.* **2022**, *55*, 84-89, <https://doi.org/10.1016/j.ifacol.2022.07.644>.
4. Raja, R.K.; Hazir, S.; Balasubramani, G.; Sivaprakash, G.; Obeth, E.S.J.; Boobalan, T.; Pugazhendhi, A.; Raj, R.H.K.; Arun, A. Chapter 22 - Green nanotechnology for the environment. In *Handbook of Microbial*

- Nanotechnology, Hussain, C.M., Ed.; Academic Press: **2022**; pp. 461-478, <https://doi.org/10.1016/B978-0-12-823426-6.00006-1>.
5. Jayasinghe, P. A., Derrible, S., & Kattan, L. Interdependencies between Urban Transport, Water, and Solid Waste Infrastructure Systems. *Infrastructures*. **2023**, 8(4), 76, <https://doi.org/10.3390/infrastructures8040076>
 6. Fu, G.; Jin, Y.; Sun, S.; Yuan, Z.; Butler, D. The role of deep learning in urban water management: A critical review. *Water Res.* **2022**, 223, 118973, <https://doi.org/10.1016/j.watres.2022.118973>.
 7. Araya, F.; Vasquez, S. Challenges, drivers, and benefits to integrated infrastructure management of water, wastewater, stormwater and transportation systems. *Sustain Cities Soc.* **2022**, 82, 103913, <https://doi.org/10.1016/J.SCS.2022.103913>.
 8. Aline, R.; Edy, L. T. M. Maria Eugenia Gimenez B. Reuse of water treatment plant sludge mixed with lateritic soil in geotechnical works. *Environ Challenges* **2022**, 7, 100465, <https://doi.org/10.1016/j.envc.2022.100465>.
 9. Panagopoulos, A. Brine management (saline water & wastewater effluents): Sustainable utilization and resource recovery strategy through Minimal and Zero Liquid Discharge (MLD & ZLD) desalination systems. *Chem Eng Process - Process Intensif.* **2022**, 176, 108944, <https://doi.org/10.1016/J.CEP.2022.108944>.
 10. Nishu, K. S. Smart and innovative nanotechnology applications for water purification. *Hybrid Adv.* **2023**, 3, 100044, <https://doi.org/10.1016/j.hybadv.2023.100044>.
 11. Sharma, S.; Dhingra, P.; Jain, S. Advancements & challenges of nanotechnology in waste water treatment. *Mater Today Proc.* **2023**, 80, 18-23, <https://doi.org/10.1016/J.MATPR.2022.09.481>.
 12. Gehrke, I.; Geiser, A. Somborn-Schulz A. Innovations in nanotechnology for water treatment. *Nanotechnol. Sci. Appl.* **2015**, 8, 1-17, <https://doi.org/10.2147/NSA.S43773>.
 13. Raouf, M.S.A.; Raheim, A.R.M.A. Removal of Heavy Metals from Industrial Waste Water by Biomass-Based Materials: A Review. *J. Pollut. Eff. Cont.* **2017**, 5, 180, <https://doi.org/10.4172/2375-4397.1000180>.
 14. Barrera, G.; Tiberto, P.; Allia, P. Magnetic properties of nanocomposites. *Appl Sci.* **2019**, 9, 212, <https://doi.org/10.3390/app9020212>.
 15. Mohammed, L.; Gomaa, H. G.; Ragab, D.; Zhu, J. Magnetic nanoparticles for environmental and biomedical applications: A review. *Particuology* **2017**, 30, 1-14, <https://doi.org/10.1016/j.partic.2016.06.001>.
 16. Jiang, B.; Lian, L.; Xing, Y. Advances of magnetic nanoparticles in environmental application: environmental remediation and (bio)sensors as case studies. *Environ. Sci. Pollut. Res.* **2018**, 25, 30863-30879, <https://doi.org/10.1007/s11356-018-3095-7>.
 17. Elakkiya, S.; Arthanareeswaran, G.; Ismail, A. F.; Goh, P.S.; Lukka, T.Y. Review on characteristics of biomaterial and nanomaterials based polymeric nanocomposite membranes for seawater treatment application. *Environ. Res.* **2021**, 197, 111177, <https://doi.org/10.1016/j.envres.2021.111177>.
 18. Schwaminger, S. P.; Syhr, C.; Berensmeier, S. Controlled synthesis of magnetic iron oxide nanoparticles: Magnetite or maghemite?. *Crystals* **2020**, 10, 214, <https://doi.org/10.3390/cryst10030214>.
 19. Dzhardimalieva, G.I.; Irzhak, V.I.; Bratskaya, S.Y. Stabilization of Magnetite Nanoparticles in Humic Acid Medium and Study of Their Sorption Properties. *Colloid. J.* **2020**, 82, 1-7, <https://doi.org/10.1134/S1061933X20010032>.
 20. Pinelli, F.; Perale, G.; Rossi, F. Coating and functionalization strategies for nanogels and nanoparticles for selective drug delivery. *Gels* **2020**, 6, 6, <https://doi.org/10.3390/gels6010006>.
 21. AL-Harbi, L.M.; Darwish, M.S.A. Functionalized iron oxide nanoparticles: synthesis through ultrasonic-assisted co-precipitation and performance as hyperthermic agents for biomedical applications. *Heliyon* **2022**, 8, e09654, <https://doi.org/10.1016/j.heliyon.2022.e09654>.
 22. Bayrakci, M.; Gezici, O.; Bas, S.Z.; Ozmen, M.; Maltas, E. Novel humic acid-bonded magnetite nanoparticles for protein immobilization. *Mater. Sci. Eng. C* **2014**, 42, 546-552, <https://doi.org/10.1016/j.msec.2014.05.066>.
 23. Shen, Y.; Jiang, B.; Xing, Y. Recent advances in the application of magnetic Fe₃O₄ nanomaterials for the removal of emerging contaminants. *Environ. Sci. Pollut. Res.* **2021**, 28, 7599-7620, <https://doi.org/10.1007/s11356-020-11877-8>.
 24. Jaeger, H.M.; He, Jinbo.; Lin, X.; McBride, S.; Barry, E.; 1. WO2013074669 - Nanoparticle-based desalination and filtration system. **2014**.

25. Veraguer, S.V.; Morales Herrero, M.P.; Pereda, C. S.; Marsansastoreca, C.; López Herrero, V. 1. WO2015177391 - Nanostructured electrolyte useful for direct osmosis desalination, method for obtaining the electrolyte and uses of same. **2015**.
26. Liu, J.F.; Zhao, Z.S.; Jiang, G.B. Coating Fe₃O₄ Magnetic Nanoparticles with Humic Acid for High Efficient Removal of Heavy Metals in Water. *Environ. Sci. Technol.* **2008**, *42*, 6949–6954, <https://doi.org/10.1021/es800924c>.
27. Qiang, S.; Yingdi, L.; Shaojun, Q.; Xiaodong, Z.; Wang, T. Preparation method for nano ferroferric oxide. **2011**.
28. Nadihya, D.; Kala, A.; Sasikumar, P.; Mohammed, M.K.; Thirunavukkarasu, P.; Prabhakaran, M.; Karnan, C.; Albukhaty, S.; Jabir, M.S.; Syed, A. Influence of Cu²⁺ substitution on the structural, optical, magnetic, and antibacterial behaviour of zinc ferrite nanoparticles. *Journal of Saudi Chemical Society* **2023**, *27*, 101696, <https://doi.org/10.1016/J.JSCS.2023.101696>.
29. Matei, E.; Predescu, A.M.; Şăulean, A.A. Ferrous Industrial Wastes—Valuable Resources for Water and Wastewater Decontamination. *Int. J. Environ. Res. Public Health* **2022**, *19*, 13951, <https://doi.org/10.3390/ijerph192113951>.
30. Janani, B.; Al-Mohaimed, A.M. Synthesis and characterizations of hybrid PEG-Fe₃O₄ nanoparticles for the efficient adsorptive removal of dye and antibacterial, and antibiofilm applications. *J. Environ. Heal. Sci. Eng.* **2021**, *19*, 389–400, <https://doi.org/10.1007/s40201-021-00612-1>.
31. Yew, Y.P.; Shameli, K.; Miyake, M. Green Synthesis of Magnetite (Fe₃O₄) Nanoparticles Using Seaweed (*Kappaphycus alvarezii*) Extract. *Nanoscale Res. Lett.* **2016**, *11*, 276, <https://doi.org/10.1186/s11671-016-1498-2>.
32. Kim, H. J.; Lee, J. M.; Choi, J. H.; Kim, D. H.; Han, G. S.; Jung, H. S. Synthesis and adsorption properties of gelatin-conjugated hematite (α -Fe₂O₃) nanoparticles for lead removal from wastewater. *J Hazard Mater.* **2021**, *416*, 125696, <https://doi.org/10.1016/j.jhazmat.2021.125696>.
33. Huang, Y.; Keller, A.A. EDTA functionalized magnetic nanoparticle sorbents for cadmium and lead contaminated water treatment. *Water Res.* **2015**, *80*, 159-168, <https://doi.org/10.1016/j.watres.2015.05.011>.
34. Gupta, A.K.; Gupta, M. Synthesis and surface engineering of iron oxide nanoparticles for biomedical applications. *Biomaterials* **2005**, *26*, 3995–4021, <https://doi.org/10.1016/j.biomaterials.2004.10.012>.
35. Heitmann, A.P.; Silva, G.C.; Paiva, P.R.P.; Dantas, M.S.S.; Ciminelli, V.S.; Souza Dinóla, I.C.; Ferreira, A.M. Magnetized manganese oxide nanocomposite for effective decontamination of Cd (II) from wastewaters. *Water Sci. Technol.* **2016**, *74*, 2762-2772, <https://doi.org/10.2166/wst.2016.446>.
36. Malik, M.; Chan, K.H.; Azimi, G. Quantification of nickel, cobalt, and manganese concentration using ultraviolet-visible spectroscopy. *RSC Adv.* **2021**, *11*, 28014-28028, <https://doi.org/10.1039/d1ra03962h>.
37. Morantes, D.; Muñoz, E.; Kam, D.; Shoseyov, O. Highly charged cellulose nanocrystals applied as a water treatment flocculant. *Nanomaterials* **2019**, *9*, 272, <https://doi.org/10.3390/nano9020272>.
38. da Silva, M.P.; de Souza, Z.S.B.; Cavalcanti, J.V.F.L.; Fraga, T.J.M.; da Motta Sobrinho, M.A.; Ghislandi, M.G. Adsorptive and photocatalytic activity of Fe₃O₄-functionalized multilayer graphene oxide in the treatment of industrial textile wastewater. *Environ. Sci. Pollut. Res.* **2021**, *28*, 23684-23698, <https://doi.org/10.1007/s11356-020-10926-6>.
39. Wojciechowska, A.; Lenzion-Bielun, Z. Synthesis and characterization of magnetic nanomaterials with adsorptive properties of arsenic ions. *Molecules* **2020**, *25*, 4117, <https://doi.org/10.3390/molecules25184117>.
40. Jain, A.; Kumari, S.; Agarwal, S.; Khan, S. Water purification via novel nano-adsorbents and their regeneration strategies. *Process Saf. Environ. Prot.* **2021**, *152*, 441–454, <https://doi.org/10.1016/j.psep.2021.06.031>.
41. Mudhoo, A.; Sillanpää, M. Magnetic nanoadsorbents for micropollutant removal in real water treatment: a review. *Environ. Chem. Lett.* **2021**, *19*, 4393–4413, <https://doi.org/10.1007/s10311-021-01289-6>.
42. Santos, A.S.G.G.; Ramalho, P.S.F.; Viana, A.T.; Lopes, A.R.; Gonçalves, A.G.; Nunes, O.C. Feasibility of using magnetic nanoparticles in water disinfection. *J. Environ. Manage.* **2021**, *288*, 112410, <https://doi.org/10.1016/j.jenvman.2021.112410>.
43. Gupta, A.K.; Berry, C.; Gupta, M.; Curtis, A. Receptor-mediated targeting of magnetic nanoparticles using insulin as a surface ligand to prevent endocytosis. *IEEE Trans Nanobiosci.* **2003**, *2*, 255-261, <https://doi.org/10.1109/TNB.2003.820279>.

44. Khurram, R.; Wang, Z.; Ehsan, M. F. α -Fe₂O₃-based nanocomposites: synthesis, characterization, and photocatalytic response towards wastewater treatment. *Environ. Sci. Pollut. Res.* **2021**, *28*, 17697–17711, <https://doi.org/10.1007/s11356-020-11778-w>.
45. Abu, E.M.; Abd-Elhamid, A.I.; Aly, H.F. Adsorption behavior of Mo(VI) from aqueous solutions using tungstate-modified magnetic nanoparticle. *Environ. Sci. Pollut. Res.* **2024**, *31*, 18900–18915, <https://doi.org/10.1007/s11356-024-32251-y>.
46. Gupta, A.K.; Wells, S. Surface-Modified Superparamagnetic Nanoparticles for Drug Delivery: Preparation, Characterization, and Cytotoxicity Studies. *IEEE Trans. Nanobiosci.* **2004**, *3*, 66–73, <https://doi.org/10.1109/TNB.2003.820277>.
47. Palit, S.; Das, P.; Basak, P. Chapter 7 - Application of nanotechnology in water and wastewater treatment and the vast vision for the future. In *3D Printing Technology for Water Treatment Applications*, Pandey, J.K., Manna, S., Patel, R.K., Qian, M., Eds.; Elsevier: **2023**; pp. 157–179, <https://doi.org/10.1016/B978-0-323-99861-1.00005-9>.
48. Alkhouzaam, A.; Qiblawey, H. Functional GO-based membranes for water treatment and desalination: Fabrication methods, performance and advantages. A review. *Chemosphere* **2021**, *274*, 129853, <https://doi.org/10.1016/j.chemosphere.2021.129853>.
49. Akintayo, C.O.; Aremu, O.H.; Igboama, W.N.; Nelana, S.M.; Ayanda, O.S. Performance evaluation of ultra-violet light and iron oxide nanoparticles for the treatment of synthetic petroleum wastewater: Kinetics of cod removal. *Materials* **2021**, *14*, 5012, <https://doi.org/10.3390/ma14175012>.
50. Azadi, F.; Karimi-Jashni, A.; Zerafat, M. M. Desalination of brackish water by gelatin-coated magnetite nanoparticles as a novel draw solute in forward osmosis process. *Environ. Technol.* **2021**, *42*, 2885–2895, <https://doi.org/10.1080/09593330.2020.1717642>.
51. Ding, G.K.C. Wastewater Treatment, Reused and Recycling – A Potential Source of Water Supply. *Ref. Module Earth Syst. Environ. Sci.* **2023**, *2*, 676–693, <https://doi.org/10.1016/B978-0-323-90386-8.00062-0>.
52. Albukhaty, S.; Sulaiman, G.M.; Al-Karagoly, H.; Mohammed, H.A.; Hassan, A.S.; Alshammari, A.A.A.; Ahmad, A.M.; Madhi, R.; Almalki, F.A.; Khashan, K.S. Iron oxide nanoparticles: The versatility of the magnetic and functionalized nanomaterials in targeting drugs, and gene deliveries with effectual magnetofection. *J. Drug Deliv. Sci. Technol.* **2024**, *99*, 105838, <https://doi.org/10.1016/J.JDDST.2024.105838>.
53. AlMalki, F.A.; Khashan, K.S.; Jabir, M.S.; Hadi, A.A.; Sulaiman, G.M.; Abdulameer, F.A.; Albukhaty, S.; Al-Karagoly, H.; Albaqami, J. Eco-friendly synthesis of carbon nanoparticles by laser ablation in water and evaluation of their antibacterial activity. *J. Nanomater.* **2022**, *2022*, 7927447, <https://doi.org/10.1155/2022/7927447>.
54. Li, Y.; Wang, J.; Li, B.; Geng, M.; Wang, Y.; Zhao, J.; Jin, B. Response of extracellular polymeric substances and microbial community structures on resistance genes expression in wastewater treatment containing copper oxide nanoparticles and humic acid. *Bioresour. Technol.* **2021**, *340*, 125741, <https://doi.org/10.1016/j.biortech.2021.125741>.
55. Dutta, D.; Das, B.M. Scope of green nanotechnology towards amalgamation of green chemistry for cleaner environment: A review on synthesis and applications of green nanoparticles. *Environ. Nanotechnol. Monit. Manag.* **2021**, *15*, 100418, <https://doi.org/10.1016/j.enmm.2020.100418>.
56. Saleh, H.M.; Albukhaty, S.; Sulaiman, G.M.; Abomughaid, M.M. Design, Preparation, and Characterization of Polycaprolactone–Chitosan Nanofibers via Electrospinning Techniques for Efficient Methylene Blue Removal from Aqueous Solutions. *J. Compos. Sci.* **2024**, *8*, 68, <https://doi.org/10.3390/jcs8020068>.

Publisher’s Note & Disclaimer

The statements, opinions, and data presented in this publication are solely those of the individual author(s) and contributor(s) and do not necessarily reflect the views of the publisher and/or the editor(s). The publisher and/or the editor(s) disclaim any responsibility for the accuracy, completeness, or reliability of the content. Neither the publisher nor the editor(s) assume any legal liability for any errors, omissions, or consequences arising from the use of the information presented in this publication. Furthermore, the publisher and/or the editor(s) disclaim any liability for any injury, damage, or loss to persons or property that may result from the use of any ideas, methods, instructions, or products mentioned in the content. Readers are encouraged to independently verify any

information before relying on it, and the publisher assumes no responsibility for any consequences arising from the use of materials contained in this publication.